

# Corrosion inhibition of carbon steel in 1 M H<sub>2</sub>SO<sub>4</sub> solution by *Thapsia villosa* extracts

A. Kalla<sup>1</sup> · M. Benahmed<sup>1</sup> · N. Djeddi<sup>1</sup> · S. Akkal<sup>2</sup> · H. Laouer<sup>3</sup>

Received: 4 October 2015 / Accepted: 16 August 2016 / Published online: 27 August 2016  
© The Author(s) 2016. This article is published with open access at Springerlink.com

**Abstract** Ethyl acetate extract (EAE) and butanolic extract (BE) of *Thapsia villosa* were investigated as corrosion inhibitors of Carbon Steel (CS) in 1 M H<sub>2</sub>SO<sub>4</sub> using electrochemical impedance spectroscopy (EIS) techniques, potentiodynamic polarization and weight loss measurements. The effect of temperature on the corrosion behavior of CS was studied in the range of 20–40 °C. The experimental results show that EAE and BE are good corrosion inhibitors and the protection efficiency increased with increasing concentration of the extracts, but decrease with rise in temperature. The EAE and BE act as a mixed types inhibitors. The adsorption of extracts on CS surface follow Langmuir isotherm. The apparent energies, enthalpies and entropies of the dissolution process were discussed.

**Keywords** Carbon steel · Corrosion · EIS · Potentiodynamic polarization · Plant extract · Weight loss

## Introduction

Metals and alloys react electrochemically with the environment to form stable compounds, in which the loss of metals occurs. Metallic structures are exposed to conditions that facilitate corrosion processes. Furthermore, hydrochloric and sulfuric acids are widely used for pickling and de-scaling of carbon steel which promote the acceleration of metallic corrosion, causing ecological risks and economic consequences in term of repair, replacement and product losses [1]. Therefore, the prevention of the corrosion is vital not only for the protection of metals but also in decreasing the dispersion of the toxic compounds into the environment [2]. One of the best-known methods for corrosion protection is the use of inhibitors [3]. Organic compounds having functional groups such as -OR, -COOH, -SR and/or NR<sub>2</sub> have been reported to inhibit corrosion of metals in acid solutions [4]. The presence of oxygen, sulfur, nitrogen atoms and multiple bonds in organic compounds enhances their adsorption ability and corrosion inhibition efficiency [1]. However, most of these compounds are expensive, toxic and not biodegradable [5]. Therefore, alternative sources of products are preferred. Investigation of plant extracts as corrosion inhibitors is interesting because they are ecologically acceptable and not expensive. Extracts of some plants such as bupleurum lancifolium [6], *Limonium thouinii* [7], and *Punica granatum* [8] have been reported to inhibit the corrosion of metals in acid solutions.

*Thapsia villosa*, which belongs to the family Apiaceae, grow over a wide area in the West Mediterranean region, including Portugal, Spain, the south of France and the North West of Africa. *Thapsia villosa* has been used in folk medicine as a purgative [9]. *Thapsia villosa* is found to contain phenylpropanoid; 2,3-dihydroxy-2-methylbutyric

✉ M. Benahmed  
riad43200@yahoo.fr

<sup>1</sup> Laboratoire des Molécules Bioactives et Applications, Université Larbi Tébessi, Route de Constantine, 12000 Tébessa, Algeria

<sup>2</sup> Laboratoire de Phytochimie et Analyses physicochimiques et Biologiques, Département de Chimie, Faculté de Sciences exactes, Université Mentouri Constantine, Route d'Ain el Bey, 25000 Constantine, Algeria

<sup>3</sup> Laboratoire de Valorisation des Ressources Naturelles Biologiques, Département de Biologie et d'écologie végétale, Université Ferhat Abbas de Sétif 1, Sétif, Algérie

acids [9], sesquiterpenes [10], terpenes [11] and essential oils [12]. However, it has never been studied for the purpose of corrosion inhibition.

The aim of this work is to investigate the inhibitory effects of ethyl acetate and *n*-butanol extracts as corrosion inhibitors for carbon steel in acidic solution using the weight loss, potentiodynamic polarization curves and electrochemical impedance measurements.

## Experimental

### Material

ASTM A179 low carbon steel composed of (wt%): C 0.11 %, Mn 0.52 %, P 0.024 %, S 0.030 % and Fe balance was used in the present study. The steel specimens were taken from the Seamless cold-drawn tube of heat exchanger for petroleum refining. Each sheet was mechanically press cut into specimens in sizes of  $3 \times 3 \times 0.2$  cm were used for gravimetric measurements, whereas specimens used for polarization and EIS measurements were imbedded in epoxy resin leaving a working area of  $1.0 \text{ cm}^2$ .

### Preparation of plant extracts

Air-dried aerial parts of *Thapsia villosa* were macerated in methyl alcohol (70 %) at room temperature. The hydro alcoholic solutions were concentrated under reduced pressure to dryness and the residue was dissolved in hot water and kept in cold overnight. After filtration, the residue was successively treated with ethyl acetate and *n*-butanol. Then, the solvents were removed to afford ethyl acetate and *n*-butanol extracts [13, 14]. The ethyl acetate extract (EAE) and *n*-butanol extracts (BE) were then used directly in the experiments.

### Solution

The aggressive solution of 1 M  $\text{H}_2\text{SO}_4$  was prepared by  $\text{H}_2\text{SO}_4$  98 % (Merck) with distilled water. The concentration range of the EAE and BE employed varied from 100 to 800 ppm.

### Electrochemical measurements

The Electrochemical experiments were carried out in the conventional three-electrode cell consisting of a CS as working electrode, a platinum rod as counter electrode and a saturated calomel electrode (SCE) as a reference electrode. Before measurement the working electrode was

immersed in test solution at open circuit potential (OCP) for 30 min to ensure OCP to reach steady state.

Electrochemical impedance spectroscopy (EIS) was carried out at the OCP of each sample was immersed for 30 min over a frequency range of 100 kHz–10 mHz with a signal amplitude perturbation of 10 mV. Inhibition efficiency ( $\eta_R$  %) was estimated using the following relation:

$$\eta_R \% = \frac{R'_p - R_p}{R'_p} \times 100 \quad (1)$$

where  $R_p$  and  $R'_p$  are polarizations resistors in the absence and presence of the inhibitor, respectively.

The potential of potentiodynamic polarization curves was started from cathodic potential of  $-250$  mV to anodic potential of  $+250$  mV vs. OCP at a sweep rate of  $1.0 \text{ mV s}^{-1}$ . Inhibition efficiency ( $\eta_p$  %) was defined as [6]:

$$\eta_p \% = \frac{i_{\text{corr}} - i'_{\text{corr}}}{i_{\text{corr}}} \times 100 \quad (2)$$

where  $i_{\text{corr}}$  and  $i'_{\text{corr}}$  represent corrosion current density values in absence and presence of inhibitor, respectively.

All electrochemical measurements were performed using a computer-controlled instrument, Voltalab-PGZ 301 with Voltmaster (ver 7.0.8) software. The above electrochemical tests were conducted for each concentration of *Thapsia villosa* extracts at different temperatures. Each experiment was repeated at least three times to check the reproducibility.

### Weight loss measurements

CS specimens were abraded with a series of SiC paper, washed with distilled water, degreased with acetone and dried with a cold air stream. Experiments were realized under total immersion in stagnant aerated condition at  $20$ – $40$  °C. The specimens were weighed and suspended in beakers. After 7 h, these coupons were taken out, washed, dried and weighed accurately. From the weight loss data, the corrosion rate (CR) was calculated from the following equation [15]:

$$\text{CR} = \frac{W}{At} \quad (3)$$

where  $W$  is the average weight loss,  $A$  is the total area of the specimen and  $t$  is immersion time (7 h). The inhibition efficiency ( $\eta_w$ ) was calculated as follows:

$$\eta_w \% = \frac{\text{CR} - \text{CR}'}{\text{CR}} \times 100 \quad (4)$$

where CR and CR' represent the values of corrosion rate in absence and presence of inhibitor respectively.

## Results and discussion

### EIS measurements

Figure 1 shows the EIS response of CS in 1 M H<sub>2</sub>SO<sub>4</sub> solution without and with various concentrations of EAE and BE at 20 °C, represented via Nyquist plots. Only one capacitive loop at the higher frequency range is observed which means that the corrosion of CS is controlled by the charge transfer process [16, 17]. The increasing diameter of loop obtained in 1 M H<sub>2</sub>SO<sub>4</sub> in the presence of EAE and BE indicated the corrosion inhibition and the strengthening of inhibitor film [18]. These loops are not perfect semi circles which can be attributed to the frequency dispersion effect as a result of the roughness and inhomogeneous of metal surface [19, 20]. Due to non-ideal frequency response the capacitance is usually replaced by a constant phase element (CPE) [19], whose impedance is given by [21]:

$$Z_{\text{CPE}} = \frac{1}{Q(j\omega)^n} \quad (5)$$

where  $Q$  is the magnitude of the CPE,  $\omega$  is the angular frequency ( $\omega = 2\pi f$ , where  $f$  is the AC frequency),  $j$  is the imaginary unit, and  $n$  is the deviation parameter of the CPE:  $0 \leq n \leq 1$ , for  $n = 1$ , Eq. (5) agrees to the impedance of an ideal capacitor, where  $Q$  is identified with the capacity.

A simple electrical equivalent circuit (EEC) has been proposed to model the experimental data. The EEC depicted in Fig. 2 is employed to analyze the impedance spectra, where  $R_1$  represents the solution resistance,  $R_2$  denotes the charge-transfer resistance, and a CPE instead of a pure capacitor represents the interfacial capacitance. The values of the interfacial capacitance  $C_{dl}$  can be calculated from CPE parameter and polarization resistor according to the following equation [22, 23]:

$$C_{dl} = R_p^{\frac{1-n}{n}} Q^{\frac{1}{n}} \quad (6)$$

where  $R_p$  is the polarization resistor. The values of parameters such as  $R_p$ ,  $Q$ ,  $n$  and  $\chi^2$ , obtained from fitting the recorded EIS as well as the derived parameters  $C_{dl}$  are listed in Table 1. The Chi-squared ( $\chi^2$ ) is used to evaluate the precision of the fitted data. Inspection of Table 1 reveals that the  $\chi^2$  values are low, which indicates that the fitted data have good agreement with the experimental data. It is observed that  $R_p$  values increased and the  $C_{dl}$  values decreased with increasing inhibitors concentration. The increase in  $R_p$  values can be attributed to the adsorption of the inhibitors on the metal surface leading to the formation of protective film on the metal surface and thus decreases the extent of the dissolution reaction [24]. The decrease in the  $C_{dl}$  values may be due to the increase in the thickness of the electric double layer [1]. The inhibition efficiency ( $\eta_p$  %) was achieved at (60 %) and (80 %) for EAE and BE, respectively.

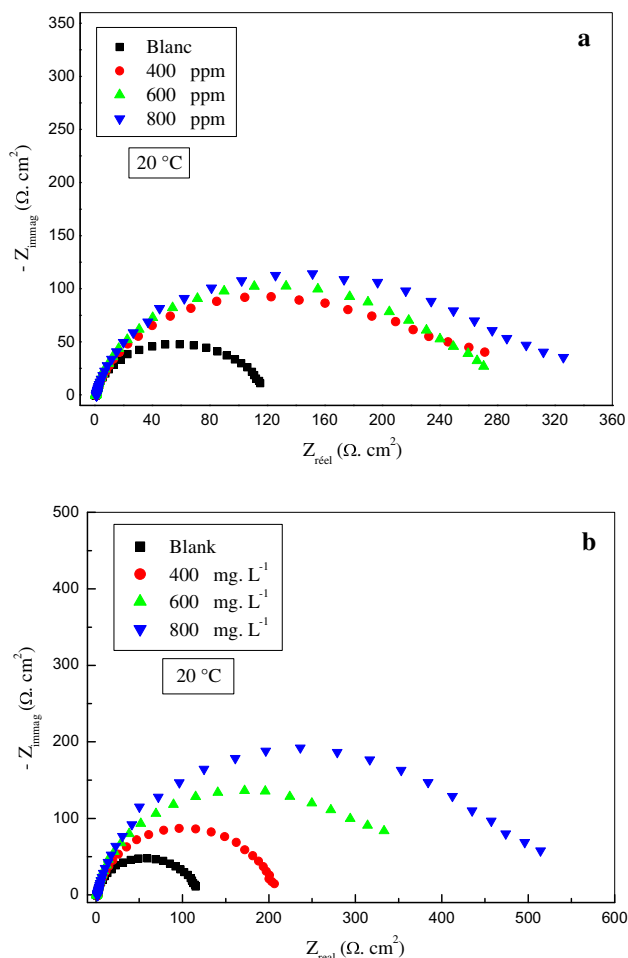


**Fig. 1** Experimental Nyquist plots for in 1 M H<sub>2</sub>SO<sub>4</sub> **a** with and without EAE, **b** with and without BE

### Potentiodynamic polarization curves

Polarization curves were obtained for CS in 1 M H<sub>2</sub>SO<sub>4</sub> solution without and with the inhibitor. Tafel plots obtained in different concentrations of EAE and BE solutions at

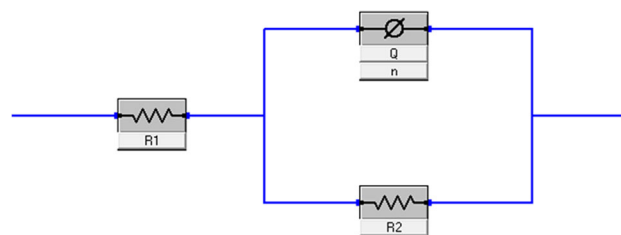


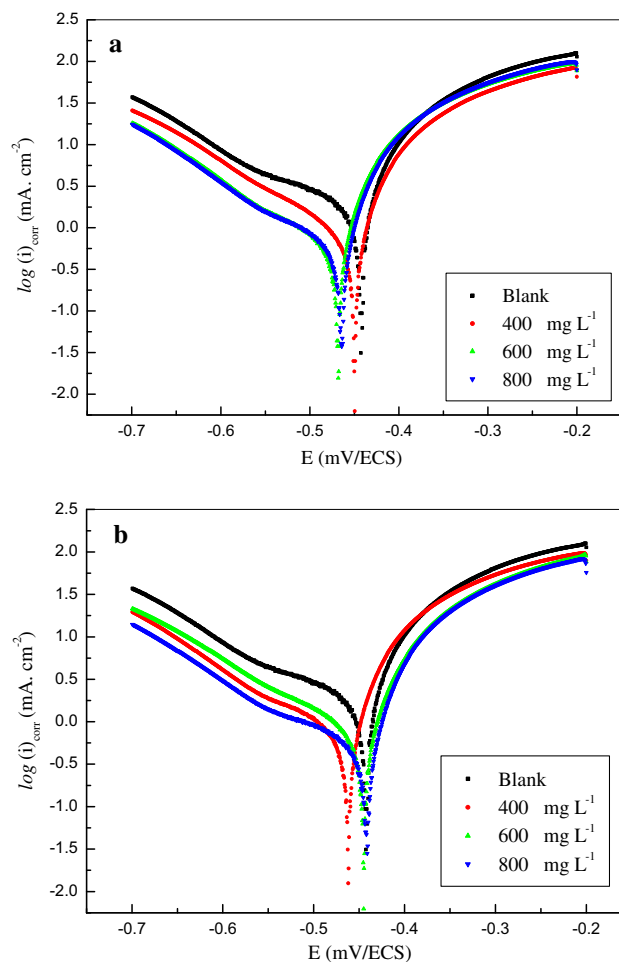
**Fig. 2** Equivalent circuit used to fit the capacitive loop

**Table 1** Impedance parameters and inhibition efficiency values for CS in 1 M H<sub>2</sub>SO<sub>4</sub> containing different concentrations of EAE and BE at 20 °C

C (ppm)	Electrochemical impedance parameters													
	EAE					BE								
	$R_p$ ( $\Omega$ cm <sup>2</sup> )	$10^4 Q$ ( $\Omega^{-1}$ S <sup>n</sup> cm <sup>-2</sup> )	$n$	$C_{dl}$ ( $\mu$ F cm <sup>-2</sup> )	$\chi^2$ ( $10^{-2}$ )	$\theta$	$\eta_R$ (%)	$R_p$ ( $\Omega$ cm <sup>2</sup> )	$10^4 Q$ ( $\Omega^{-1}$ S <sup>n</sup> cm <sup>-2</sup> )	$n$	$C_{dl}$ ( $\mu$ F cm <sup>-2</sup> )	$\chi^2$ ( $10^{-2}$ )	$\theta$	$\eta_R$ (%)
0	129.5	10.34	0.715	287	1.38	–	–	129.5	10.34	0.715	287	1.38	–	–
400	270.0	7.46	0.765	139	0.58	0.5203	52.03	301.1	4.20	0.865	125	0.52	0.5699	56.99
600	293.4	4.42	0.864	128	1.05	0.5586	55.86	387.3	4.22	0.781	95	1.50	0.6656	66.56
800	331.2	1.94	0.882	114	0.55	0.6090	60.90	488.5	1.65	0.758	75	0.69	0.7349	73.49

20 °C were shown in Fig. 3. The electrochemical parameters including corrosion potential ( $E_{corr}$ ), corrosion current density ( $i_{corr}$ ), anodic and cathodic Tafel slopes ( $\beta_a$  and  $\beta_c$ ), surface coverage values ( $\theta$ ) and inhibition efficiency ( $\eta_p = \theta \times 100$ ) are presented in Table 2.

It is clear from Fig. 3 and Table 2 that, the addition of both EAE and BE to the acid solution causes a remarkable decrease in the corrosion rate predominantly shifts the cathodic curves to lower values of current densities; it may be due to the adsorption of organic compounds present in the extracts at the active sites of CS surface, retarding both metallic dissolution and hydrogen evolution reactions and consequently slowed down the corrosion process [25]. The structure and functional groups of the inhibitors play prominent roles during the adsorption process [1]. Inspection of Table 2 showed that both anodic and cathodic Tafel slopes do not change remarkably upon addition of EAE and BE, which indicates that the extracts act as a mixed type inhibitor for the corrosion of C steel. The values of inhibition efficiency ( $\eta_p$ %) determined using potentiodynamic

**Fig. 3** Potentiodynamic polarization curves for CS in 1 M H<sub>2</sub>SO<sub>4</sub> **a** with and without EAE, **b** with and without BE

**Table 2** Polarization parameters and corresponding inhibition efficiency for the corrosion of CS in 1 M H<sub>2</sub>SO<sub>4</sub> containing different concentrations of EAE and BE at 20 °C

C (ppm)	Polarization parameters					EAE					BE							
	$i_{corr}$ (mA cm <sup>-2</sup> )	$E_{corr}$ (mV)	$\beta_a$ (mV dec <sup>-1</sup> )	$\beta_c$ (mV dec <sup>-1</sup> )	$\theta$	$\eta_p$ (%)	$i_{corr}$ (mA cm <sup>-2</sup> )	$E_{corr}$ (mV)	$\beta_a$ (mV dec <sup>-1</sup> )	$\beta_c$ (mV dec <sup>-1</sup> )	$\theta$	$\eta_p$ (%)	$i_{corr}$ (mA cm <sup>-2</sup> )	$E_{corr}$ (mV)	$\beta_a$ (mV dec <sup>-1</sup> )	$\beta_c$ (mV dec <sup>-1</sup> )	$\theta$	$\eta_p$ (%)
0	1.0308	441.2	42.4	109.1	–	–	1.0308	441.2	42.4	109.1	–	–	1.0308	441.2	42.4	109.1	–	–
400	0.5052	501.3	46.7	75.6	0.5099	50.99	0.4405	460.6	37.6	99.0	0.5727	57.27	0.4405	460.6	37.6	99.0	0.5727	57.27
600	0.4565	458.7	37.9	72.6	0.5571	55.71	0.3780	443.7	41.3	94.5	0.6333	63.33	0.3780	443.7	41.3	94.5	0.6333	63.33
800	0.4082	463.1	37.4	70.3	0.6040	60.40	0.2671	440.3	37.6	92.3	0.7409	74.09	0.2671	440.3	37.6	92.3	0.7409	74.09

polarization are in good agreement with those obtained from EIS measurements.

**Weight loss measurements**

*Effect of concentration and temperature on corrosion rate and inhibition efficiency*

The weight loss expressed as the corrosion rate (CR) for the CS specimens in 1 M H<sub>2</sub>SO<sub>4</sub> solution containing different concentrations of *Thapsia villosa* extracts (EAE and BE) as a function of inhibitor concentration in the temperature range of 20–40 °C is showed in Fig. 4. Inspection of the plots revealed that CR decreases noticeably with increase in both of EAE and BE concentrations, indicating that the addition of plant extracts retard the dissolution process of CS.

In similar experimental conditions, the influence of temperature on CR was studied. The results presented in the Table 3 and Fig. 4 show that the CR increases with temperature both in uninhibited and inhibited solutions,

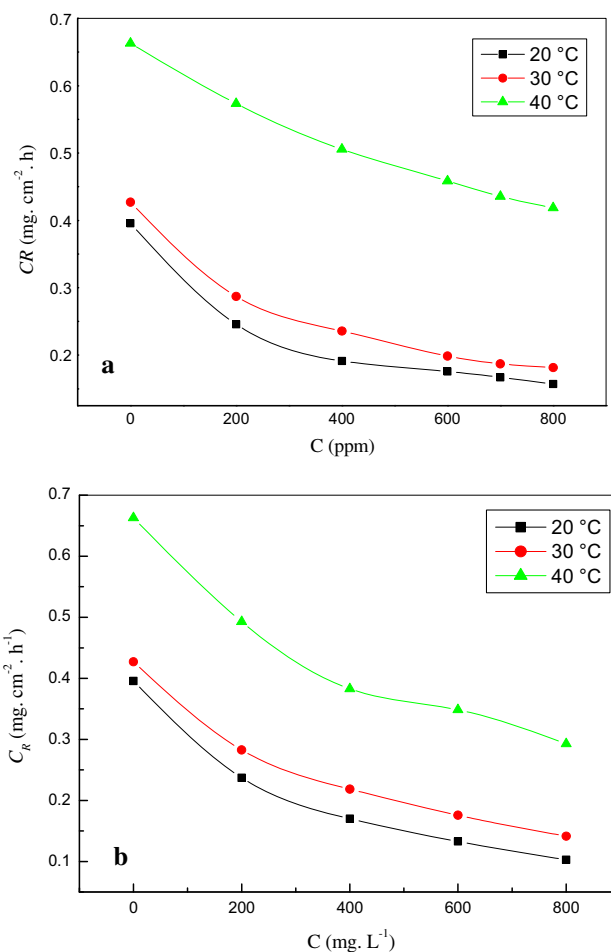


**Fig. 4** Relationship between corrosion rate and concentration of: **a** EAE in 1 M H<sub>2</sub>SO<sub>4</sub>, **b** BE in 1 M H<sub>2</sub>SO<sub>4</sub>

**Table 3** Corrosion parameters obtained from weight loss of CS in 1 M H<sub>2</sub>SO<sub>4</sub> containing various concentrations of EAE and BE at different temperatures

	C (ppm)	Temperature (°C)								
		20			30			40		
		CR (mg cm <sup>-2</sup> h <sup>-1</sup> )	$\theta$	$\eta_w$ (%)	CR (mg cm <sup>-2</sup> h <sup>-1</sup> )	$\theta$	$\eta_w$ (%)	CR (mg cm <sup>-2</sup> h <sup>-1</sup> )	$\theta$	$\eta_w$ (%)
EAE	Blank	0.3957	–	–	0.4271	–	–	0.663	–	–
	200	0.2457	0.3791	37.91	0.2871	0.3278	32.78	0.5734	0.1351	13.51
	400	0.1914	0.5163	51.63	0.2357	0.4481	44.81	0.5057	0.2372	23.72
	600	0.1757	0.5560	55.60	0.1986	0.5350	53.50	0.4586	0.3083	30.83
	700	0.1671	0.5777	57.77	0.1871	0.5619	56.19	0.4357	0.3428	34.28
	800	0.1571	0.6030	60.30	0.1814	0.5753	57.53	0.4186	0.3686	36.86
BE	Blank	0.3957	–	–	0.4271	–	–	0.663	–	–
	200	0.2371	0.4008	40.08	0.2828	0.3378	33.78	0.4928	0.2567	25.67
	400	0.1700	0.5704	57.04	0.2186	0.4882	48.82	0.3828	0.3567	35.67
	600	0.1328	0.6644	66.44	0.1757	0.5886	58.86	0.3486	0.4742	47.42
	800	0.1028	0.7402	74.02	0.1414	0.6689	66.89	0.2928	0.5583	55.83
	800	0.1028	0.7402	74.02	0.1414	0.6689	66.89	0.2928	0.5583	55.83

and goes up more rapidly at the higher temperature; the rise in temperature usually accelerates the corrosion reactions which results in higher dissolution rates of the metal.

The variation of inhibition efficiency ( $\eta_w$ %) with temperature and plant extracts concentrations is shown in Table 3 and Fig. 5. It is clear from Fig. 5 that  $\eta_w$ % increases with the increase in EAE and BE concentration, while it decreased with increase in temperature. This can be attributed to increased rate of desorption of phytochemical compounds from the surface of CS with increasing temperature because these two opposite processes are in equilibrium [26, 27]. Several authors have reported similar observation and the plant extracts were believed to be physically adsorbed on the CS surface [26, 28, 29].

At the EAE concentration of 800 ppm, the maximum EI % in 1 M H<sub>2</sub>SO<sub>4</sub> is 60 % at 20 °C; 57 % at 30 °C; and 37 % at 40 °C. While at the same concentration of BE, the maximum EI % in 1 M H<sub>2</sub>SO<sub>4</sub> is 74 % at 20 °C; 67 % at 30 °C; and 56 % at 40 °C. The results indicate that both extracts are good inhibitors for CS in 1 M H<sub>2</sub>SO<sub>4</sub> solution and the maximum inhibition efficiency was achieved using BE.

#### Adsorption isotherm

The decrease in CR by addition of EAE and BE is attributed to either adsorption of the plant component on the CS surface [30]. To evaluate the adsorption process of phytochemical components on the CS surface, Langmuir,

Temkin and Freundlich isotherms were obtained according to following equations:

$$\text{Langmuir: } \frac{C}{\theta} = \frac{1}{K_{\text{ads}}} + C \quad (7)$$

$$\text{Temkin: } \theta = \frac{1}{\alpha} \log K_{\text{ads}} C \quad (8)$$

$$\text{Freundlich: } \log \theta = \log K_{\text{ads}} + \alpha \log C \quad (9)$$

where:  $C$  is the concentration of inhibitor,  $K_{\text{ads}}$  is the adsorption equilibrium constant,  $\theta$  is the surface coverage,  $\alpha$  is the adsorbate parameter

The correlation coefficient ( $r^2$ ), presented in the Table 4, was used to choose the isotherm that best fit experimental data. Best results from the plots were obtained for Langmuir adsorption isotherm, that suggests monolayer adsorption of both EAE and BE on the CS surface at all temperatures.

Figure 6a, b show the straight lines of  $C/\theta$  versus  $C$ , deviate from unity for EAE at 20–40 °C, indicates that the interaction force between phytochemical compounds on the CS surface cannot be neglected [28, 31], and each molecule occupies more than one adsorption site on the metal surface [32]. A modified Langmuir adsorption isotherm could be applied to this phenomenon, which is given by following equation [33]:

$$\frac{C}{\theta} = \frac{n}{K_{\text{ads}}} + nC \quad (10)$$

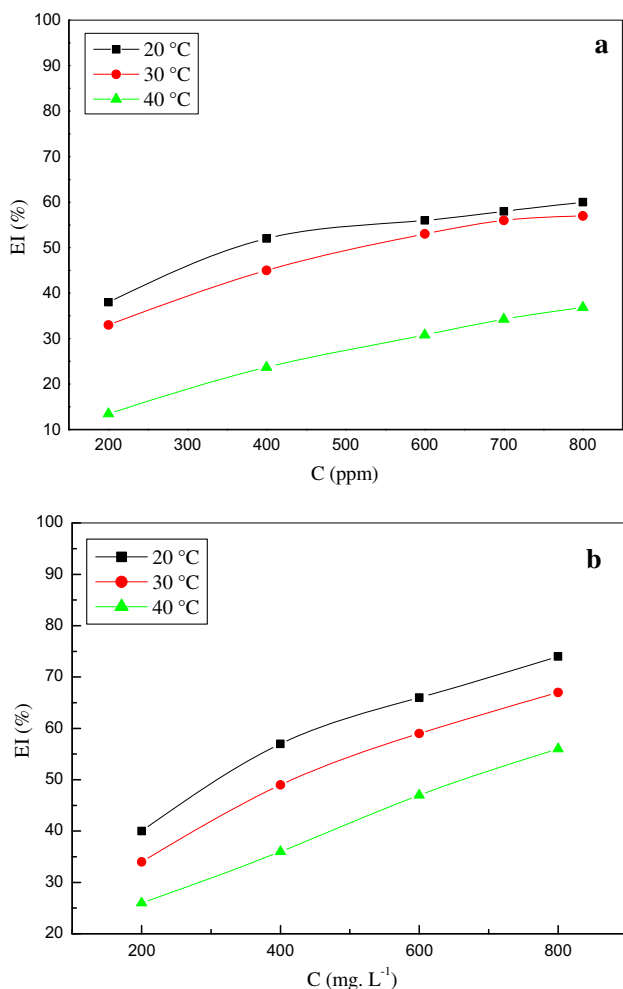


**Fig. 5** Effect of temperature and concentration on the inhibition efficiency of: **a** EAE in 1 M H<sub>2</sub>SO<sub>4</sub>, **b** BE in 1 M H<sub>2</sub>SO<sub>4</sub>

**Table 4** Correlation coefficient (*r*<sup>2</sup>)

Isotherm	EAE			BE		
	20 °C	30 °C	40 °C	20 °C	30 °C	40 °C
Langmuir	0.999	0.999	0.999	0.999	0.999	0.998
Temkin	0.991	0.998	0.997	0.936	0.990	0.978
Freundlich	0.984	0.976	0.998	0.997	0.997	0.966

**Table 5** Parameters of the linear regression between *C*/*θ* and *C* in 1 M H<sub>2</sub>SO<sub>4</sub>

<i>T</i> (°C)	Parameters of the linear regression					
	EAE			BE		
	Slope	<i>r</i> <sup>2</sup>	<i>K</i> <sub>ads</sub> (L mg <sup>-1</sup> )	Slope	<i>r</i> <sup>2</sup>	<i>K</i> <sub>ads</sub> (L mg <sup>-1</sup> )
20	1.36	0.999	5.47 × 10 <sup>-3</sup>	0.93	0.999	3.09 × 10 <sup>-3</sup>
30	1.27	0.999	3.49 × 10 <sup>-3</sup>	1.02	0.999	2.51 × 10 <sup>-3</sup>
40	1.15	0.999	0.93 × 10 <sup>-3</sup>	1.08	0.998	1.64 × 10 <sup>-3</sup>

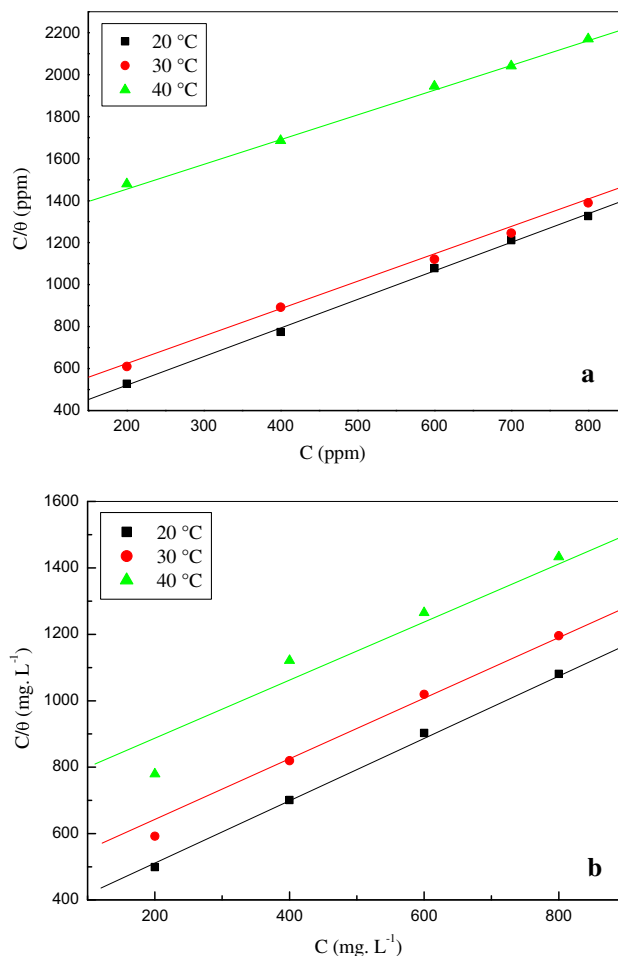


**Fig. 6** Langmuir isotherm adsorption for CS in 1 M H<sub>2</sub>SO<sub>4</sub> at different temperatures of **a** the EAE **b** of the BE

On the contrary, for the BE, the slope almost equals to unity, which suggests that the interaction of adsorbed species is negligible [34].

The adsorptive equilibrium constant (*K*<sub>ads</sub>) listed in Table 5 was estimated from intercept of the Langmuir isotherm plot. The values of equilibrium constant decrease with rise in temperature, which may be attributed to desorption of inhibitor components at higher temperature [35, 36].

**Table 6** Polarization parameters and corresponding inhibition efficiency for the corrosion of CS in 1 M H<sub>2</sub>SO<sub>4</sub> without and with EAE and BE at (20–40) °C

T (°C)	C (ppm)	EAE					BE						
		$i_{\text{corr}}$ (mA cm <sup>-2</sup> )	$\beta_a$ (mV dec <sup>-1</sup> )	$-\beta_c$ (mV dec <sup>-1</sup> )	$\theta$	$\eta_p$ (%)	$C$ ppm	$-E_{\text{corr}}$ (mV)	$i_{\text{corr}}$ (mA cm <sup>-2</sup> )	$\beta_a$ (mV dec <sup>-1</sup> )	$-\beta_c$ (mV dec <sup>-1</sup> )	$\theta$	$\eta_p$ (%)
20	Blank	441.2	1.0308	42.4	109.1	–	0	441.2	1.0308	42.4	109.1	–	–
	800	463.1	0.4082	37.4	70.3	0.6040	800	440.9	0.2700	37.6	92.3	0.7403	74
30	Blank	430.8	1.0998	43.8	136.0	–	0	430.8	1.0998	43.8	136.0	–	–
	800	425.3	0.4710	66.5	54.2	0.5717	800	471.1	0.3483	34.6	94.2	0.6689	66.89
40	Blank	430.0	1.1019	48.0	137.7	–	0	430.0	1.1019	48.0	137.7	–	–
	800	422.2	0.7017	45.6	108.0	0.3632	800	451.0	0.4630	39.8	96.4	0.5583	55.83

**Table 7** Impedance parameters and inhibition efficiency values for CS without and with EAE and BE at (20–40) °C

T (°C)	C (ppm)	EAE					BE							
		$R_p$ ( $\Omega$ cm <sup>2</sup> )	$10 Q$ ( $\Omega^{-1} S^0$ cm <sup>-2</sup> )	$n$	$C_{dl}$ ( $\mu F$ cm <sup>-2</sup> )	$\chi^2$ ( $10^{-2}$ ) <sup>2</sup>	$\theta$	$\eta_R$ (%)	$R_p$ ( $\Omega$ cm <sup>2</sup> )	$10^4 Q \Omega^{-1} S^0$ cm <sup>-2</sup> )	$n$	$C_{dl}$ ( $\mu F$ cm <sup>-2</sup> )	$\chi^2$ ( $10^{-2}$ ) <sup>2</sup>	$\theta$
20	Blank	129.5	10.34	0.715	287	1.38	–	129.5	10.34	0.715	287	1.38	–	–
	800	331.2	1.94	0.882	114	0.55	0.6090	651.4	1.10	0.755	60	0.70	0.8012	75.12
30	Blank	110.5	10.60	0.717	302	2.14	–	110.5	10.60	0.717	302	2.14	–	–
	800	264.0	2.32	0.827	129	1.04	0.5814	357.9	1.98	0.700	91	1.73	0.6912	69.12
40	Blank	92.42	13.0	0.684	314	1.85	–	80.42	13.0	0.684	314	1.85	–	–
	800	144.6	6.01	0.620	201	0.87	0.3608	188.3	7.02	0.712	133	1.30	0.5729	57.29





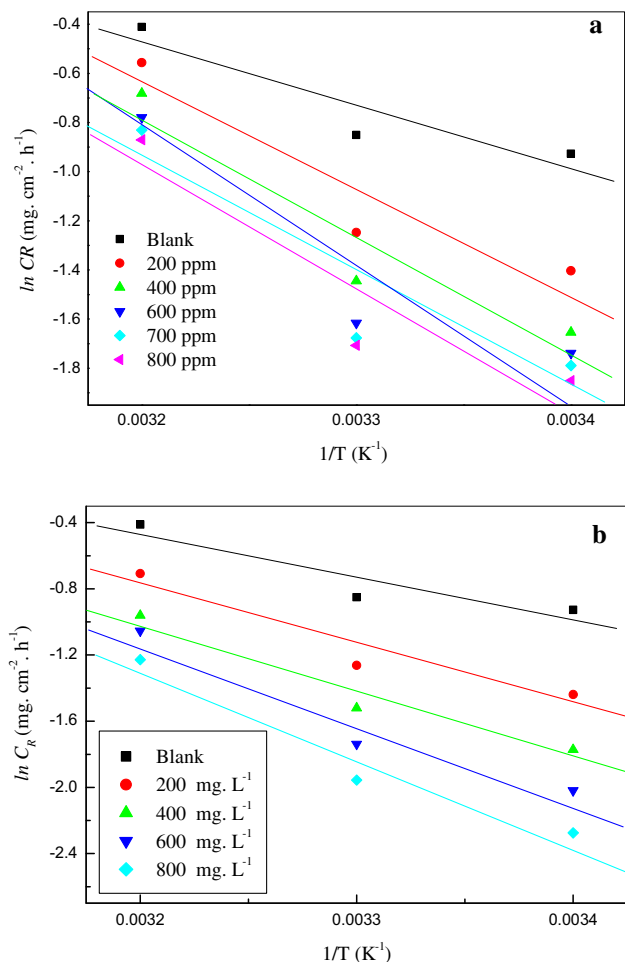


**Fig. 7** Arrhenius plots related to the corrosion rate for CS in 1 M H<sub>2</sub>SO<sub>4</sub> **a** EAE, **b** BE

*Effect of the temperature*

The effect of temperature on the rate of the CS corrosion process using electrochemical measurements was studied in 1 M H<sub>2</sub>SO<sub>4</sub> alone and in the presence of EAE and BE. Corresponding data are given in Tables 6 and 7. It was

found that the corrosion current density (*i*<sub>corr</sub>) increased but the polarization resistance (*R*<sub>p</sub>) and the inhibition efficiency decreased with increasing temperature. The decrease in inhibition efficiency reveals that the film formed on the metal surface is less protective at higher temperatures, since desorption rate of the inhibitor is greater at higher temperatures [37].

The activation parameters were calculated from Arrhenius equation:

$$CR = A \exp\left(-\frac{E_a^\circ}{RT}\right) \tag{11}$$

where CR is corrosion rate, *E*<sub>a</sub><sup>°</sup> is the apparent activation energy of the CS dissolution and *A* is the Arrhenius pre-exponential factor. The apparent activation energy was calculated from the plots of logarithm of CR versus 1/*T* (Fig. 7) and shown in Table 8. It can be seen in the Table 8 that *E*<sub>a</sub><sup>°</sup> is higher in the presence of the inhibitors than in their absence and increased with the increase in concentration of EAE and BE, which indicate a strong adsorption of the inhibitor molecules at the CS surface [1].

An alternative form of Arrhenius equation is the transition-state equation [38, 39]:

$$CR = \frac{RT}{N_A h} \exp\left(\frac{\eta S_a^\circ}{R}\right) \exp\left(-\frac{\eta H_a^\circ}{RT}\right) \tag{12}$$

where *h* is the plank’s constant, *N*<sub>A</sub> is Avogadro’s number, *ηS*<sub>a</sub><sup>°</sup> the entropy of activation and *ηH*<sub>a</sub><sup>°</sup> is the enthalpy of activation. Figure 8 shows a plot of *ln*CR/*T* vs. 1/*T*. Straight lines were obtained with a slope of  $-\frac{\eta H_a^\circ}{RT}$  and an intercepts of  $\left(\ln \frac{R}{N_A h} + \frac{\eta S_a^\circ}{R}\right)$ , from which the values of *ηS*<sub>a</sub><sup>°</sup> and *ηH*<sub>a</sub><sup>°</sup> were calculated and listed in Table 8. For both ethyl acetate and *n*-butanol extracts, the positive signs of enthalpies reflect the endothermic nature of the dissolution process [39, 40].

**Table 8** The values of activation parameters *E*<sub>a</sub><sup>°</sup>, *ΔH*<sub>a</sub><sup>°</sup> and *ΔS*<sub>a</sub><sup>°</sup> for CS in 1 M H<sub>2</sub>SO<sub>4</sub> at different concentrations of EAE and BE at different temperatures

C (ppm)	EAE			BE		
	<i>E</i> <sub>a</sub> <sup>°</sup> (kJ mol <sup>-1</sup> )	<i>ΔH</i> <sub>a</sub> <sup>°</sup> (kJ mol <sup>-1</sup> )	<i>ΔS</i> <sub>a</sub> <sup>°</sup> (J mol <sup>-1</sup> K <sup>-1</sup> )	<i>E</i> <sub>a</sub> <sup>°</sup> (kJ mol <sup>-1</sup> )	<i>ΔH</i> <sub>a</sub> <sup>°</sup> (kJ mol <sup>-1</sup> )	<i>ΔS</i> <sub>a</sub> <sup>°</sup> (J mol <sup>-1</sup> K <sup>-1</sup> )
Blank	21.45	18.71	−15.58	21.45	18.71	−15.58
200	35.23	32.49	27.06	30.42	27.69	10.59
400	40.39	37.64	42.49	33.74	31.00	19.25
600	39.88	37.13	39.82	40.12	37.37	38.74
800	39.84	37.09	39.24	43.51	40.76	48.13
1000	–	–	–	51.73	48.98	74.01

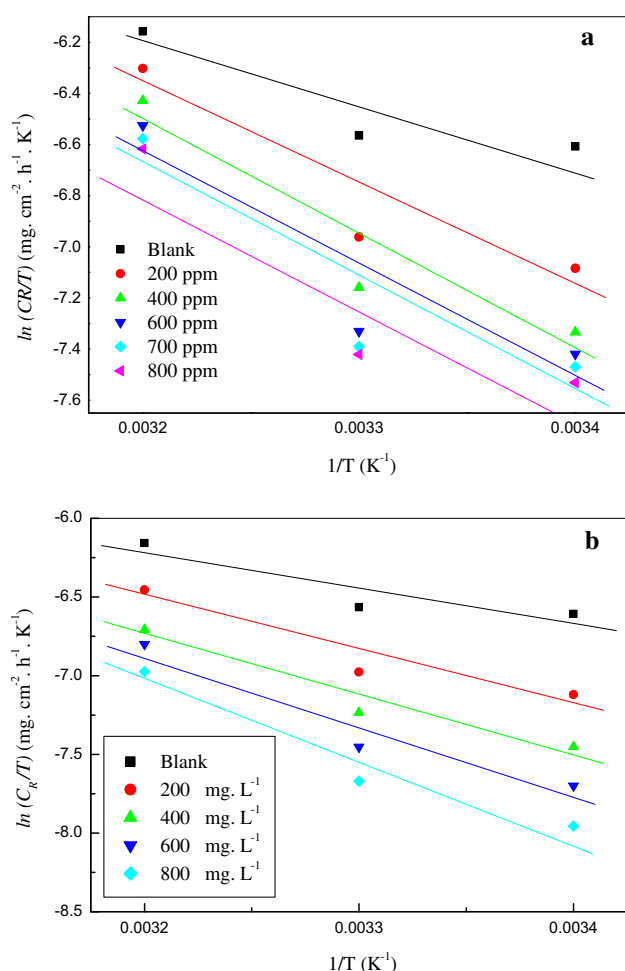


**Fig. 8** Arrhenius plots of corrosion  $\ln(CR/T)$  vs.  $1/T$  for CS in 1 M  $H_2SO_4$  **a** with and without EAE, **b** with and without BE

It is evident from data listed in Table 8 that, the values of  $E_a^0$  are larger than corresponding values of  $\eta H_a^0$  indicating the corrosion process involved a gaseous reaction, simply the hydrogen evolution reaction, associated with a decrease in total reaction volume [39, 40]. Moreover, the difference value  $E_a^0 - \eta H_a^0$  is 2.74 kJ/mol, which is approximately equal to the average value of  $RT$ . Therefore, this shows that the corrosion process is a unimolecular reaction as it is characterized by the equation:

$$E_a^0 - \eta H_a^0 = RT \quad (13)$$

Investigation of Table 8 reveals that the sign of  $\eta S_a^\circ$  is negative in free acid solution, whereas it becomes positive with the addition of both extracts, this suggest that the adsorption of organic inhibitor molecules is accompanied by desorption of water molecules from the steel surface [41]. Hence, the gain in entropy is attributed to the increase in solvent entropy and to more positive water desorption enthalpy [26]. The positive values of the entropy, related to

substitutional adsorption, can be attributed more to the increase of adsorbed inhibitor molecules rather than the decrease of water molecule desorption [41].

## Conclusion

It can be concluded as follows:

- EAE and BE of *Thapsia villosa* act as good inhibitors for the corrosion of CS in 1 M  $H_2SO_4$  solution.
- The inhibition efficiency of all electrochemical tests and weight loss measurements were in good agreement.
- The inhibition efficiency of CS in acid solution increased with increases in concentrations of the EAE and BE and decreases with rising temperature.
- The adsorption of organic molecules on the CS surface obeys the Langmuir adsorption isotherm.
- Potentiodynamic polarization measurements demonstrate that EAE and BE act as a mixed-type inhibitions.
- The apparent activation energy ( $E_a$ ) of CS dissolution increases in presence of *Thapsia villosa* extracts.

**Open Access** This article is distributed under the terms of the Creative Commons Attribution 4.0 International License (<http://creativecommons.org/licenses/by/4.0/>), which permits unrestricted use, distribution, and reproduction in any medium, provided you give appropriate credit to the original author(s) and the source, provide a link to the Creative Commons license, and indicate if changes were made.

## References

1. Kumar CBP, Mohana KN (2014) Corrosion inhibition efficiency and adsorption characteristics of some Schiff bases at mild steel/hydrochloric acid interface. *J Taiwan Inst Chem Eng* 45:1031–1042
2. Solmaz R (2010) Investigation of the inhibition effect of 5-((E)-4-phenylbuta-1,3-dienylideneamino)-1,3,4-thiadiazole-2-thiol Schiff base on mild steel corrosion in hydrochloric acid. *Corros Sci* 52:3321–3330
3. Doner A, Sahin EA, Kardas G et al (2013) Investigation of corrosion inhibition effect of 3-[(2-hydroxybenzylidene)-amino]-2-thioxio-thiazolidin-4-one on corrosion of mild steel in the acidic medium. *Corros Sci* 66:278–284
4. Abiola OK, Tobun Y (2010) *Cocos nucifera* L. water as green corrosion inhibitor for acid corrosion of aluminium in HCl solution. *Chin Chem Lett* 21:1449–1452
5. Chevalier M, Robert F, Amusant N et al (2014) Enhanced corrosion resistance of mild steel in 1 M hydrochloric acid solution by alkaloids extract from *Aniba rosaedora* plant: electrochemical, phytochemical and XPS studies. *Electrochim Acta* 131:96–105
6. Benahmed M, Selatnia I, Achouri A et al (2015) Steel corrosion inhibition by *Bupleurum lancifolium* (Apiaceae) extract in acid solution. *Trans Indian Inst Met* 68:393–401
7. Benahmed M, Lafhal M, Djeddi N et al (2012) Inhibition of the corrosion of carbon steel in acid solution by the extract of *Limonium thouinii* (Plumbaginaceae). *Adv Environ Biol* 6:4052–4056



8. Behpour M, Ghoreishi SM, Khyatkashani M et al (2012) Green approach to corrosion inhibition of mild steel in two acidic solutions by the extract of *Punica granatum* peel and main constituents. Mater Chem Phys 131:621–633
9. Teresa JDP, Pascual MD, Arias A et al (1985) Helmanticine, a phenylpropanoid from *Thapsia villosa*. Phytochemistry 24(8):1773–1778
10. Rubal JJ, Guerra FM, Moreno-Dorado FJ et al (2004) Sulfur-containing sesquiterpenes from *Thapsia villosa*. Tetrahedron 60:159–164
11. Lemmich E, Smitt UW, Jensen JS et al (1991) Guaiane esters from *Thapsia villosa*. Phytochemistry 30:2987–2990
12. Avato P, Trabace G, Smitt UW (1996) Essential oils from fruits of three types of *Thapsia villosa*. Phytochemistry 43:609–612
13. Benahmed M, Akkal S, Louaar S et al (2006) A new furanocoumarin glycoside from *Carum montanum* (Apiaceae). Biochem Syst Ecol 34:645–647
14. Benahmed M, Akkal S, Elomri A et al (2014) Constituents from *Bupleurum montanum* (Coss. & Dur.) (Apiaceae). Arab J Chem 7:1065–1069
15. Djeddi N, Benahmed M, Makhloufi E et al (2015) Study on methylene dichloride and butanolic extracts of *Reutera lutea* (Desf.) Maire (Apiaceae) as effective corrosion inhibitors for carbon steel in HCl solution. Res Chem Intermed 41:4595–4616
16. Raja PB, Qureshi AK, Rahim AA et al (2013) *Neolamarckia cadamba* alkaloids as eco-friendly corrosion inhibitors for mild steel in 1 M HCl media. Corros Sci 69:292–301
17. Tang Y, Zhang F, Hu S et al (2013) Novel benzimidazole derivatives as corrosion inhibitors of mild steel in the acidic media. Part I: gravimetric, electrochemical, SEM and XPS studies. Corros Sci 74:271–282
18. Muthukrishnan P, Jeyaprabha B, Prakash P (2013) Adsorption and corrosion inhibiting behavior of *Lannea coromandelica* leaf extract on mild steel corrosion. Arab J Chem 7:1065–1069
19. Li L, Zhang X, Lei J et al (2012) Adsorption and corrosion inhibition of *Osmanthus fragran* leaves extract on carbon steel. Corros Sci 63:82–90
20. Shuduan D, Li X (2012) Inhibition by Ginkgo leaves extract of the corrosion of steel in HCl and H<sub>2</sub>SO<sub>4</sub> solutions. Corros Sci 55:407–415
21. Qian B, Hou B, Zheng M (2013) The inhibition effect of tannic acid on mild steel corrosion in seawater wet/dry cyclic conditions. Corros Sci 72:1–9
22. Lebrini M, Robert F, Lecante A et al (2011) Corrosion inhibition of C38 steel in 1 M hydrochloric acid medium by alkaloids extract from *Oxandra asbeckil* plant. Corros Sci 53:687–695
23. Lecante A, Robert F, Blandinières PA et al (2011) Anti-corrosive properties of *S. tinctoria* and *G. ouregou* alkaloid extracts on low carbon steel. Curr Appl Phys 11:714–724
24. Bentiss F, Traisnel M, Lagrenee M (2000) The substituted 1,3,4-oxadiazoles: a new class of corrosion inhibitors of mild steel in acidic media. Corros Sci 42:127–146
25. Torres VV, Amado RS, de Sá CF et al (2011) Inhibitory action of aqueous coffee ground extracts on the corrosion of carbon steel in HCl solution. Corros Sci 53:2385–2392
26. Ramya K, Mohan R, Anupama KK et al (2015) Electrochemical and theoretical studies on the synergistic interaction and corrosion inhibition of alkyl benzimidazoles and thiosemicarbazide pair on mild steel in hydrochloric acid. Mater Chem Phys 14(9–150):632–647
27. Nazeer AA, Shalabi K, Fouda AS (2015) Corrosion inhibition of carbon steel by Roselle extract in hydrochloric acid: electrochemical and surface study. Res Chem Intermed 41:4833–4850
28. Odewunmi NA, Umoren SA, Gasem ZM (2015) Watermelon waste products as green corrosion inhibitors for mild steel in HCl solution. J Environ Chem Eng 3:286–296
29. Eduok UM, Khaled M (2015) Corrosion inhibition for low-carbon steel in 1 M H<sub>2</sub>SO<sub>4</sub> solution by phenytoin: evaluation of the inhibition potency of another “anticorrosive drug”. Res Chem Intermed 41:6309–6324
30. Rochdi A, Tourir R, Bakri ME (2015) Protection of low carbon steel by oxadiazole derivatives and biocide against corrosion in simulated cooling water system. J Environ Chem Eng 3:233–242
31. Mu GN, Li XH, Qu Q et al (2006) Molybdate and tungstate as corrosion inhibitors for cold rolling steel in hydrochloric acid solution. Corros Sci 48:445–459
32. Obot IB, Umoren SA, Gasem ZM et al (2015) Theoretical prediction and electrochemical evaluation of vinylimidazole as corrosion inhibitors for mild steel in 1 M HCl. J Ind Eng Chem 21:1328–1339
33. Vilamiml RFV, Corio P, Rubin JC et al (1999) Effect of sodium dodecylsulfate on copper corrosion in sulfuric acid media in the absence and presence of benzotriazole. J Electroanal Chem 472:112
34. Li X, Deng S, Fu H et al (2014) Synergistic inhibition effects of bamboo leaf extract/major components and iodide ion on the corrosion of steel in H<sub>3</sub>PO<sub>4</sub> solution. Corros Sci 78:29–42
35. Li X, Deng S, Xie X (2014) Inhibition effect of tetradecylpyridinium bromide on the corrosion of cold rolled steel in 7.0 M H<sub>3</sub>PO<sub>4</sub>. Arab J Chem. doi:10.1016/j.arabjc.2014.05.004
36. Desimone MP, Gordillo G, Simison SN (2011) The effect of temperature and concentration on the corrosion inhibition mechanism of an amphiphilic amido-amine in CO<sub>2</sub> saturated solution. Corros Sci 53:4033–4043
37. El-Haddad MN (2014) Hydroxyethylcellulose used as an eco-friendly inhibitor for 1018 C-steel corrosion in 3.5% NaCl solution. Carbohydr Polym 112:595–602
38. Tebbji K, Faska N, Tounsi A et al (2007) The effect of some lactones as inhibitors for the corrosion of mild steel in 1 M hydrochloric acid. Mater Chem Phys 106:260–267
39. Hamdy A, El-Gendy NS (2013) Thermodynamic, adsorption and electrochemical studies for corrosion inhibition of carbon steel by henna extract in acid medium. Egypt J Pet 22:17–25
40. Ostovari A, Hoseinie SM, Peikari M et al (2009) Corrosion inhibition of mild steel in 1 M HCl solution by henna extract: a comparative study of the inhibition by henna and its constituents (Lawson, Gallic acid, Glucose and Tannic acid). Corros Sci 51:1935–1949
41. Moretti G, Guidi E, Fabris F (2013) Corrosion inhibition of the mild steel in 0.5 M HCl by 2-butyl-hexahydropyrrrol [1,2-b][1,2]oxazole. Corros Sci 76:206–218

